

# Amphiphile micelles formed by polystyrene/poly(2-vinyl pyridine) heteroarm star copolymers in toluene

D. Voulgaris<sup>a</sup>, C. Tsitsilianis<sup>a,\*</sup>, V. Grayer<sup>b</sup>, F.J. Esselink<sup>b</sup>, G. Hadziioannou<sup>b</sup>

<sup>a</sup>Department of Chemical Engineering, University of Patras, and Institute of Chemical Engineering and High Temperature Chemical Processes, ICE/HT-FORT, P.O. Box 1414, 26500 Patras, Greece

<sup>b</sup>Department of Polymer Chemistry and Material Science Center, University of Groningen, Nijenborg 4, 9747 AG Groningen, The Netherlands

Received 24 August 1998; received in revised form 18 November 1998; accepted 18 November 1998

## Abstract

We report the micellar behavior of polystyrene/poly(2-vinyl pyridine) heteroarm star copolymers ( $PS_nP2VP_n$ ) in toluene which is a selective solvent of polystyrene. A series of  $PS_nP2VP_n$  were synthesized by anionic polymerization and their micellar characteristics such as critical micelle concentrations (cmc), aggregation numbers, hydrodynamic dimensions and core–corona sizes were determined by the means of static and dynamic light scattering, viscometry and transmission electron microscopy. All these parameters were studied as a function of the insoluble arm length and the corresponding scaling relations were established. Our system seems to belong to the class of *amphiphile micelles* characterized by strong dependencies of the aggregation number and the microdomain sizes on the insoluble arm length. This behavior is also characteristic of strongly segregated diblock and triblock copolymer systems. © 1999 Elsevier Science Ltd. All rights reserved.

**Keywords:** Heteroarm star copolymers; Amphiphile micelles; Scaling relations

## 1. Introduction

Micellization phenomena taking place in block copolymers immersed in a selective solvent have been the subject of extensive studies in the last decades [1–6]. Most of the theoretical and experimental work had been devoted to linear diblock and triblock copolymers. In recent years block copolymers exhibiting more complex architecture such as heteroarm star [7–10], functionalized star [11] and super H [12] have attracted much attention targeting the elucidation of the effect of macromolecular architecture on the association phenomena.

In a previous article the association behavior of a polystyrene/poly(2-vinylpyridine) ( $PS_nP2VP_n$ ) heteroarm star copolymer was examined in toluene which is a selective solvent for PS and its behavior was compared to that of the corresponding diblock copolymer, the blocks of which have the same degree of polymerization as the different arms of the star [9].

It was shown that star molecules bearing 6 PS and 6 P2VP arms of symmetrical length radiating from a small and tight poly(divinylbenzene) nodule, undergo association following the closed association model. The so formed micelles

adopt a core-shell structure of spherical shape the core radius of which is almost equal with the corona thickness (Fig. 1).

The influence of architecture on micellization phenomena is significant as it arises from comparing the behavior of the heteroarm star and the corresponding diblock. The critical micelle concentrations (cmc) of the  $A_nB_n$  star copolymer is three orders of magnitude higher the cmc of the linear AB homologue and its aggregation number is about one order of magnitude lower.

In the present communication, we study the influence of the insoluble arm length on the micellar association of heteroarm star copolymers in a selective solvent. A number of characteristics of the micelles, such as the aggregation number ( $N_{agg}$ ), the hydrodynamic radius ( $R_H$ ) etc. were measured for  $PS_nP2VP_n$  star copolymers in toluene as a function of the number of P2VP repeat units keeping both the number of arms  $n$  and the length of the soluble PS arms constant. The established scaling relationships are discussed in the frame of the existing theories concerning block copolymers. Our system seems to belong to the category of *amphiphile micelles* also formed by strongly segregated diblock and triblock copolymer systems. The particularities of this class of micelles are thoroughly discussed in a recent article of Forster et al. [13].

\* Corresponding author.

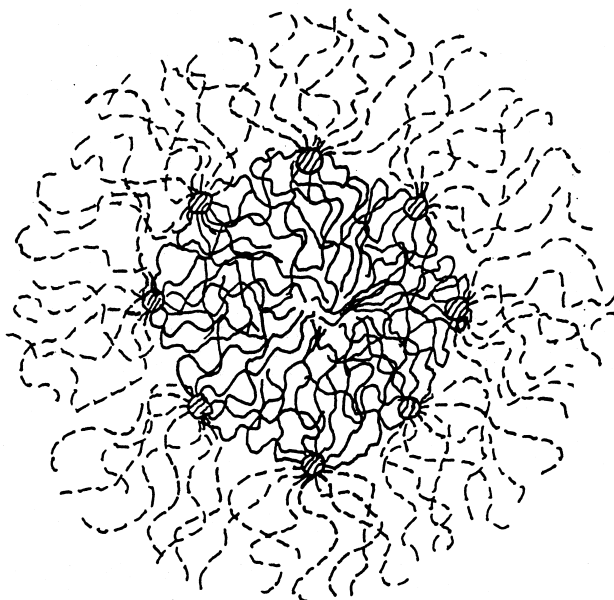


Fig. 1. Schematical presentation of a polymolecular micelle which was formed by a heteroarm star copolymer  $PS_nP2VP_6$  in toluene.

The article is organized in three parts. First we present the influence of the insoluble arm length (P2VP) of the heteroarm star copolymer on cmc and the aggregation number by using static light scattering, after we determine the hydrodynamic dimensions of the micelles by viscometry and dynamic light scattering and we discuss their dependencies from the P2VP arm length and finally we look at the core size and corona thickness with the aid of transmission electron microscopy.

## 2. Experimental part

### 2.1. Materials

The  $PS_nP2VP_n$  star copolymers were prepared via anionic polymerization under argon atmosphere using THF as solvent. The procedure used, is a three step sequential «living» copolymerization [14] which allows the preparation of a series of samples differing only in the length of the second generation of arms (e.g. P2VP) from the same reaction.

In the first step, the PS arms are synthesized, a number of which are joined together in the second step by reacting the living PS chains with a small amount of divinylbenzene. A star-shaped polystyrene ( $PS_n$ ) is thus formed, bearing a number of active sites on its poly(divinylbenzene) nodule which is equal to the number of the attached PS arms. In the third step a second generation of P2VP arms are growing from the nodules by adding the vinyl pyridine (VP) in the reaction medium. In this step parts of the reaction mixture were withdrawn following every addition of another amount of the VP monomer. Therefore for a given  $PS_n$  star a series of three heteroarm stars was obtained with different P2VP arm lengths. This procedure provides that all the other molecular characteristics of the samples are precisely the same. Another sample with slightly different number of arms and PS arm length has also incorporated in the present study. The small differences in its molecular characteristics with the others lie within the experimental error and their influence on the scaling relationships can be considered negligible as it was caused by regression analysis.

All the samples became free from PS precursor residuals

Table 1  
Molecular characteristics of  $PS_nP2VP_n$  heteroarm star copolymers

Sample <sup>a</sup>	$M_w \times 10^{-4}$ PS arm	$M_w/M_n$ PS arm	$M_w \times 10^{-5}$ $PS_n$	$M_w \times 10^{-5}$ $PS_nP2VP_n$	$W_{P2VP}$ (%) (NMR)	$N_{P2VP}$ <sup>b</sup> P2VP arm	$n^c$
167 <sub>6</sub> -148 <sub>6</sub>	2.0	1.15	1.54	2.49	44	148	6.9
167 <sub>6</sub> -282 <sub>6</sub>	2.0	1.15	1.54	4.39	60	282	6.9
167 <sub>6</sub> -365 <sub>6</sub>	2.0	1.15	1.54	5.44	66	365	6.9
205 <sub>6</sub> -240 <sub>6</sub>	2.3	1.08	1.50	3.29	53	240	6.3

<sup>a</sup> The numbers indicate  $N_{PS}$  and  $N_{P2VP}$  of the corresponding arms and subscript the arm functionality.

<sup>b</sup> By the formula:  $N_{P2VP} = \{M_n(PS_{arm}) + m_{DVB}[DVB]/[LE]\} \cdot W_{P2VP} / (1 - W_{P2VP}) \cdot m_{2VP}$ .

<sup>c</sup> Average functionality:  $n = M_w(PS_n) / \{M_w(PS_{arm}) + m_{DVB}[DVB]/[LE]\}$  where  $[DVB]/[LE]$  is the divinylbenzene per living ends mole ratio.

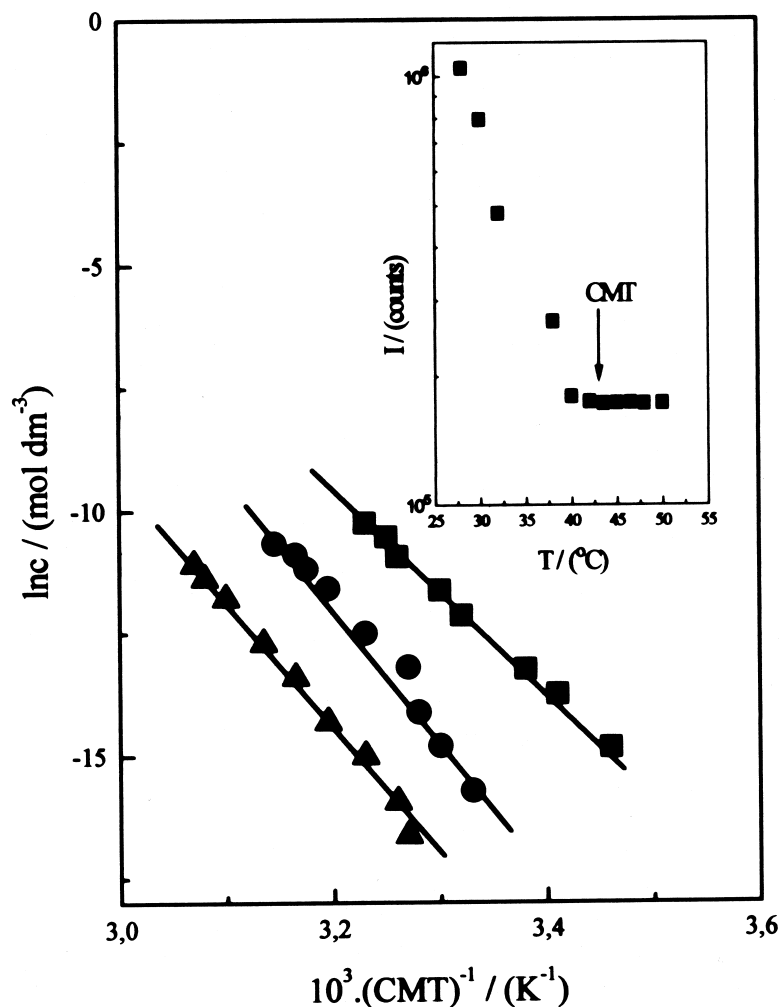


Fig. 2. Plots of the logarithm of the concentration as a function of the reciprocal of the critical micelle temperature for 167<sub>6</sub>-148<sub>6</sub> (■), 167<sub>6</sub>-282<sub>6</sub> (●) and 167<sub>6</sub>-365<sub>6</sub> (▲) samples. The inset demonstrates the determination of critical micelle temperature: plot of the light scattering intensity as a function of the temperature.

and were characterized by the means of light scattering (LS),  $H^1$  NMR and gel permeation chromatography (GPC). Their molecular characteristics are collected in Table 1. Details of the synthesis and the characterization are reported elsewhere [14].

## 2.2. Light scattering

Static and dynamic light scattering were carried out in toluene using a thermally regulated ( $\pm 0.1^\circ\text{C}$ ) spectrogoniometer model SEM RD (Sematech, France) equipped with an He–Ne laser (633 nm). The required refractive index increments  $dn/dc$  values were measured by a Chromatic KMX-16 differential refractometer operating at 633 nm.

The dynamic light scattering measurements were performed by the means of a R.T.G. correlator (Sematech, France). Correlation functions were analyzed to second order by the method of cumulants. The scattering angle used was  $90^\circ$  (angular dependence was negligible) and the pinhole was 200  $\mu\text{m}$ .

The polymer solutions were heated at  $80^\circ\text{C}$  overnight and allowed to equilibrate at room temperature. Prior to the measurements the solutions were made free from foreign particles by filtration with 0.45  $\mu\text{m}$  filters. The temperature during the measurements was controlled to  $20^\circ\text{C}$ .

## 2.3. Viscometry

Viscometric measurements were carried out with a Schott-Gerate AVS-300 automated viscosity measuring system using Ubbelohde-type dilution viscometers in a thermally regulated ( $\pm 0.05^\circ\text{C}$ ) water bath. Intrinsic viscosities ( $\eta$ ) were obtained using Huggins plots according to the equation:

$$\eta_{sp}/c = [\eta] + K_H[\eta]^2c, \quad (1)$$

where  $\eta_{sp}/c$  is the reduced viscosity,  $K_H$  the Huggins coefficient and  $c$  the polymer concentration in  $\text{g cm}^{-3}$ .

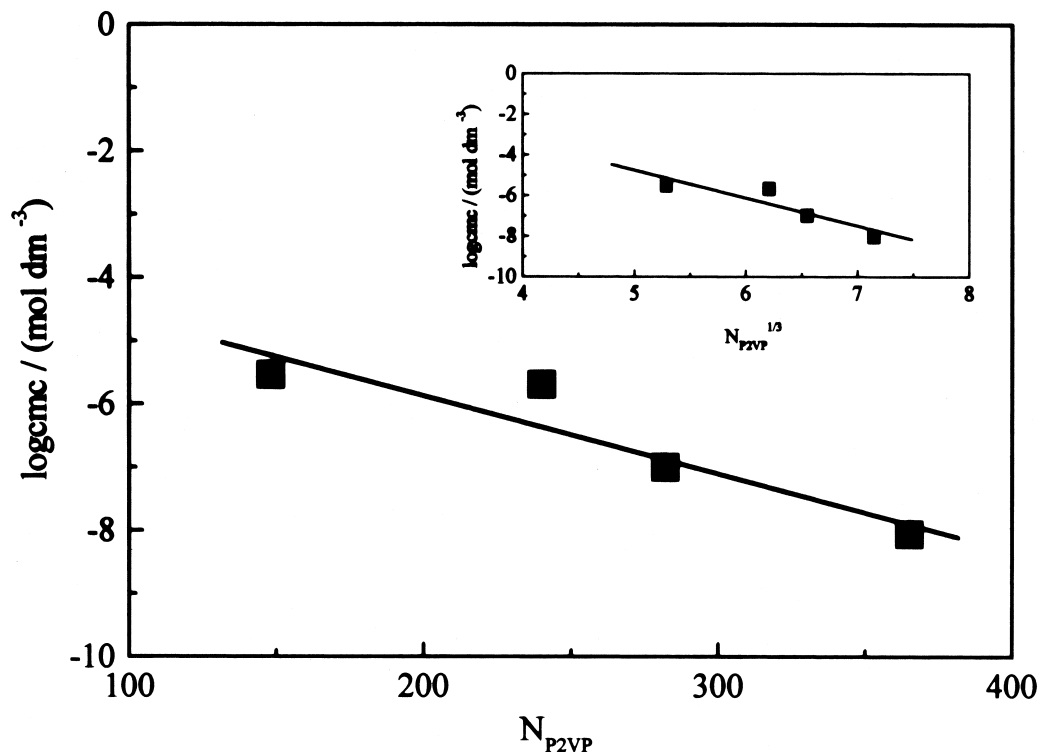


Fig. 3. Plot of the logarithm of the critical micelle concentration at 25°C as a function of the insoluble arm length. The inset presents the linear dependence of the logarithm of the critical micelle concentration at 25°C from the cubic root of the insoluble arm length.

#### 2.4. Microscopy

The morphology of the  $PS_nP2VP_n$  star copolymer micelles were obtained by transmission electron microscopy. All experiments were done with the aid of a JEOL 1200-EX Electron Microscope which was operated at 100 kV.

All the polymer samples were cast from dilute solutions in toluene while they were stained with iodine at room temperature. A droplet of the solution was put on a normal carbon-coated copper grid and subsequently blotted with help of a small filter paper. The films were allowed to dry several hours before use.

### 3. Results and discussion

#### 3.1. Critical micelle concentrations and aggregation numbers

Static light scattering was used to determine the cmc for a number of  $PS_nP2VP_n$  samples differing only on the number of the VP repeat units. The determination of cmc from the classical plots of the concentration dependencies of the reduced inverse scattering intensities was not possible as the cmc of  $PS_nP2VP_n$  copolymers with high P2VP content are lower than the experimentally accessible polymer concentrations at 25°C.

Alternatively, the critical micelle temperatures (cmt) can

be observed for all the samples. The cmt is defined as the temperature at which the appearance of the micelles can just be detected experimentally. A representative plot for the cmt determination is presented in the inset of Fig. 2. Light scattering intensities obtained at 90° are plotted as a function of temperature for a given concentration of a  $PS_nP2VP_n$  sample in toluene. The cmt is taken as the temperature below which the intensity starts to increase (indicated by the arrow).

We have shown previously that Eq. (2) is valid for the system under investigation [9]:

$$d \ln(\text{cmc})/dT^{-1} = d \ln c/d(\text{cmt})^{-1}. \quad (2)$$

Thus, in order to determine the cmc for all the samples at 25°C, cmt were recorded for a number of concentrations.

In Fig. 2  $\ln c$  is plotted as a function of the reciprocal of cmt. Straight lines were obtained with regression factors greater than 0.98 in all cases. The equations of these lines can be used to determine cmc for a given temperature.

The cmc values at 25°C were plotted as a function of the degree of polymerization of the insoluble arm,  $N_{P2VP}$  in Fig. 3. A monotonous decrease of cmc with increasing  $N_{P2VP}$  can be observed. Obviously when the length of the insoluble P2VP arms of the heteroarm star copolymer increases the solubility of the molecule decreases and the onset of micellization occurs at lower concentrations.

In order to compare our results with those concerning diblock copolymers we use the mixed micelle model

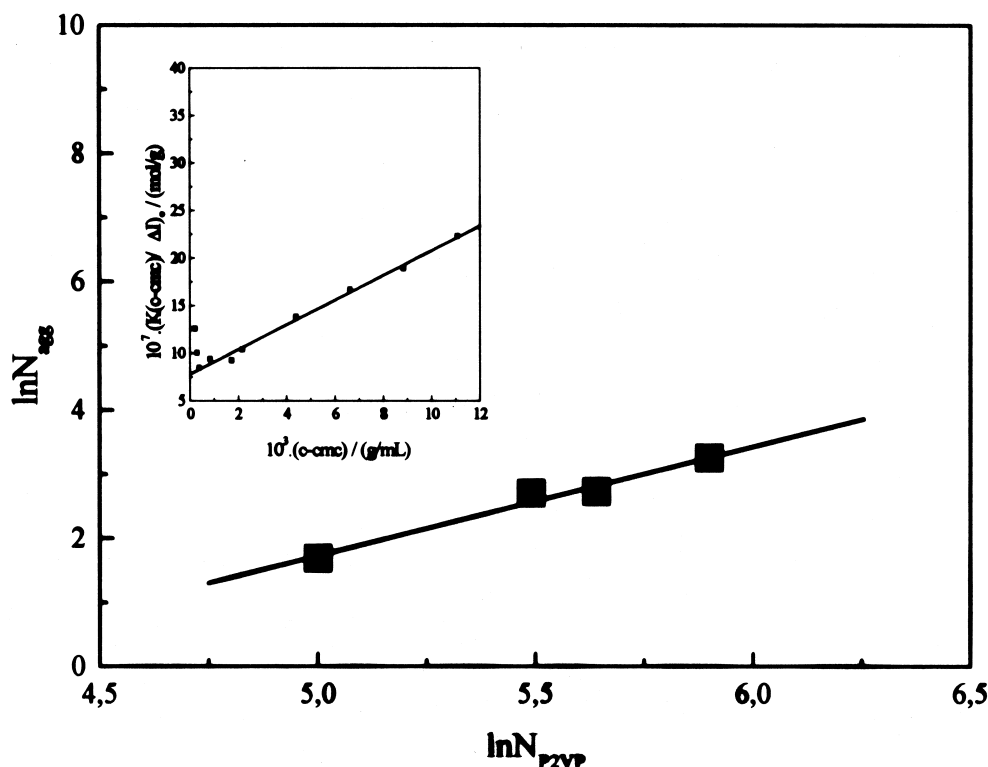


Fig. 4. Linear dependence of the logarithm of the aggregation number from the logarithm of the insoluble arm length. The inset demonstrates the determination of the  $M_w$  of the micelles.

proposed by Gao and Eisenberg [15]. According to this model, the cmc for a monodisperse block copolymer is given as

$$\log \text{cmc} = aN^{1/3} + b, \quad (3)$$

where  $a$  and  $b$  are constants and  $N$  is the number of repeat units in the insoluble block.

In the inset of Fig. 3 the data were plotted according to Eq. (3). A satisfactory linear regression ( $r = 0.90$ ) can be seen. The constants  $a$  and  $b$  were determined as  $-1.38$  and  $2.10$ , respectively.

As a result of the absence of constants  $a$  and  $b$  for the corresponding PS–P2VP diblock copolymer/toluene system we could compare our results with those of the similar PS–P4VP/toluene system where  $a$ ,  $b$  are  $-1.66$  and  $-0.9$ , respectively [16]. The lower values of the slope  $a$  indicates that the dependence of the cmc on the length of the insoluble block is somewhat weaker for the heteroarm star. However, as it arises from the difference in the constant  $b$  the cmc values for the star copolymer are three orders of magnitude higher than those of the linear copolymer, corroborating our previous findings [9].

As we have determined the cmc values at  $25^\circ\text{C}$  the standard Gibbs energy of micellization,  $\Delta G^0$ , can also be evaluated using the equation

$$\Delta G^0 \cong RT \ln(\text{cmc}). \quad (4)$$

A weak dependence of  $\Delta G^0$  on the insoluble arm length was observed. As the insoluble arm length increases,  $\Delta G^0$  becomes more negative implying that micellization is getting more favorable.

In order to evaluate the aggregation numbers,  $N_{\text{agg}}$ , of the  $\text{PS}_n\text{P2VP}_n$  micelles we have treated the light scattering data according to Zimm procedure by using the equation

$$\frac{K(c - \text{cmc})}{\Delta I} = \frac{1}{M_w P_\theta} + 2A_2(c - \text{cmc}), \quad (5)$$

where  $K$  is the optical constant,  $\Delta I$  the difference between the scattering intensity of the solution and that of the «solvent» (solution at cmc),  $P_\theta$  the particle scattering function,  $M_w$  the apparent molecular weight of the scattering particles,  $A_2$  the second virial coefficient and  $c$  the polymer concentration.

Inverse scattering intensities extrapolated to zero angle,  $(Kc/\Delta I)_0$  were plotted as a function of concentrations. An example is depicted in the inset of Fig. 4. The apparent  $M_w$  of the micelles were obtained by extrapolation to zero concentration at the region where the equilibrium between micelles and unimers were shifted in favor of micelles. In this region we have assumed that free remaining unimers do not contribute significantly to the scattering intensity. As the  $dn/dc$  values for the PS and P2VP in toluene are close to each other, possible compositional heterogeneity of the copolymers does not influence the determination of  $M_w$ . In this respect, the apparent values of  $M_w$  are very close to the

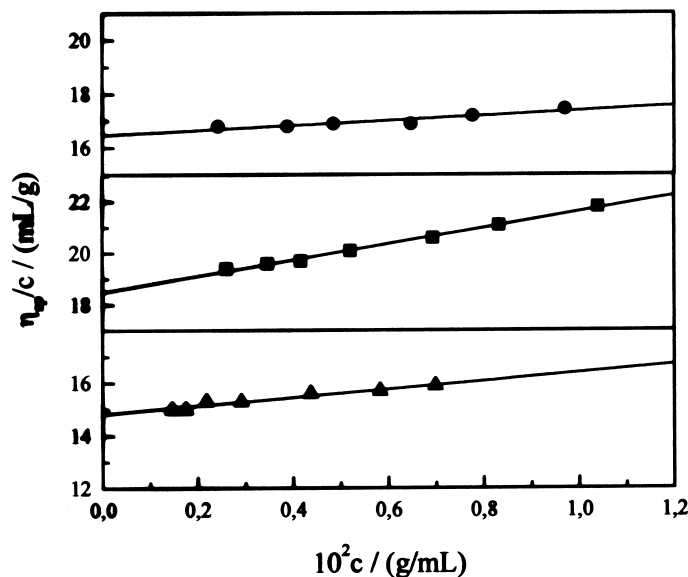


Fig. 5. Concentration dependence of the reduced specific viscosity of 167<sub>6</sub>-148<sub>6</sub> (■), 167<sub>6</sub>-282<sub>6</sub> (●) and 167<sub>6</sub>-365<sub>6</sub> (▲) samples at 20°C.

true molecular weight of the micelles. The aggregation number,  $N_{\text{agg}}$  can thus be estimated by dividing the  $M_w$  of the micelle with that of the unimer. The dependence of  $N_{\text{agg}}$  on the degree of polymerization of the different blocks of the copolymers can be described by scaling relations of the type

$$N_{\text{agg}} \sim N_{\text{P2VP}}^\alpha N_{\text{PS}}^{-\beta}, \quad (6)$$

where  $N_{\text{P2VP}}$  and  $N_{\text{PS}}$  are the number of repeat units of the insoluble and soluble block, respectively. As we have kept  $N_{\text{PS}}$  constant, scaling relations of the type  $N_{\text{agg}} \sim N_{\text{P2VP}}^\alpha$  can be derived.

In Fig. 4 a double logarithmic plot of  $N_{\text{agg}}$  as a function of  $N_{\text{P2VP}}$  is illustrated. A linear regression (with regression coefficient  $r = 0.99$ ) yields a scaling relation with exponent  $\alpha = 1.71$ . The magnitude of the exponent  $\alpha$  is a characteristic for the thermodynamic state of the system [13]. Three types of micelles can be distinguished each of which exhibits the following scaling relations

$$N_{\text{agg}} \sim N^{4/5} \text{ hairy micelle,}$$

$$N_{\text{agg}} \sim N^1 \text{ crew cut micelle,} \quad (7)$$

$$N_{\text{agg}} \sim N^2 \text{ amphiphile micelle,}$$

where *hairy micelles* are the micelles with the corona much larger than the core, *crew-cut micelles* with core much larger than the corona and *amphiphile micelles* which are formed by amphiphilic block copolymers characterized by large interaction parameter  $\chi_{\text{AB}}$ . The latter implies strong segregation between the A and B blocks. Moreover amphiphile micelles characterize a thermodynamic state where spherical micelles are always in the equilibrium structure.

Our case resembles *amphiphile micelles*. The value of the

exponent  $\alpha$  is large and close to two which is the theoretical value characteristic for this class of micelles [17]. Moreover the  $\chi N$  parameters ( $\chi$  is the Flory–Huggins interaction parameter between the different monomers and  $N = N_A + N_B$ ). The  $\chi$  value was taken from the relation  $\chi(T) = 91.6/T - 0.095$  valid for PS–P2VP diblock copolymers) for all the samples at 25°C lie in the range between 66 and 111 [18] implying a strong segregated system ( $\chi N \gg 10$ ).

A nearly  $N_{\text{P4VP}}^2$  dependence was observed in the similar PS–P4VP/toluene system for diblock copolymers. The  $\alpha$  exponent in that case is 1.91, slightly higher than in our case [13].

### 3.2. Hydrodynamic dimensions

In order to determine the hydrodynamic dimensions of the micelles, viscometry and dynamic light scattering were employed.

Intrinsic viscosities,  $[\eta]$  were obtained from the linear extrapolation of the reduced viscosities,  $\eta_{\text{sp}}/c$  to zero concentrations, using Huggins plots (Eq. (1)) as depicted in Fig. 5. The viscometric hydrodynamic radius,  $R_v$ , were calculated using the equation

$$R_v = (3[\eta]M_w/10\pi N_{\text{av}})^{1/3}, \quad (8)$$

where  $N_{\text{av}}$  is the Avagadro number and  $M_w$  is the molecular weight of the micelles. All the data are collected in Table 2.

The dependence of  $R_v$  on the insoluble arm length is also demonstrated in the form of a scaling relation. In Fig. 6  $\ln R_v$  is plotted as a function of  $\ln N_{\text{P2VP}}$ . A linear regression ( $r = 0.99$ ) through the points gave  $R_v \sim N_{\text{P2VP}}^{0.8}$ .

The hydrodynamic radius  $R_H$  were determined from dynamic light scattering measurements. Translational diffusion coefficients extrapolated to zero concentrations,  $D_0$ ,

Table 2  
Hydrodynamic characteristics of PS<sub>n</sub>P2VP<sub>n</sub> heteroarm copolymer micelles in toluene

Sample	$[\eta]$ (ml/g)	$M_w \times 10^{-6}$	$R_v$ (nm)	$D_0 \times 10^7$ (cm <sup>2</sup> /s)	$R_H$ (nm)	$R_v/R_H$
167 <sub>6</sub> -148 <sub>6</sub>	18.5	1.27	15	2.394	14	1.07
205 <sub>6</sub> -240 <sub>6</sub>	19.0	4.95	25	1.477	25	1.00
167 <sub>6</sub> -282 <sub>6</sub>	16.5	6.48	26	1.408	26	1.00
167 <sub>6</sub> -365 <sub>6</sub>	14.8	14.16	32	1.174	31	1.03

were obtained according to the formula

$$D = D_0(1 + K_D c), \quad (9)$$

where  $K_D$  is the diffusion virial coefficient and  $c$  the concentration. A typical plot of the diffusion coefficients  $D$  versus  $c$  is depicted in the inset of Fig. 7. As it is shown all the points fit in a straight line as micelles predominate in that region of concentrations. Moreover the linearity is an indication of the existence of stable structures.  $R_H$  were calculated according to the Stokes–Einstein equation

$$R_H = kT/6\pi\eta_s D_0, \quad (10)$$

where  $k$  is the Boltzmann constant,  $T$  the absolute temperature and  $\eta_s$  the viscosity of the solvent.  $R_H$  values are included in Table 2. The ratios of the viscometric to the hydrodynamic radius  $R_v/R_H$  are close to unity, a value which is expected for spherical particles. This is in agreement with the morphology observations (described in the following section) and the exponent characterizing the variation of  $N_{agg}$  with  $N_{P2VP}$ .

The influence of the length of the insoluble arms on  $R_H$  again is described by a double logarithmic plot of  $R_H$  versus  $N_{P2VP}$  (Fig. 7).

As expected the overall size of the micelles increases with increasing the length of the insoluble arms and this is because of the fact that the aggregation number also increases with  $N_{P2VP}$ . This implies that there should be a relation between the  $N_{P2VP}$  dependence of  $R_H$  and  $N_{agg}$ .

Linear regression of the data gave  $R_H \sim N_{P2VP}^{0.89}$  ( $r = 0.98$ ). For simple space filling arguments we may say that  $R_H \sim N_{agg}^{1/3} N_{P2VP}^{1/3}$  and if  $N_{agg} \sim N_{P2VP}^a$  then the domain

size scales as  $R_H \sim N_{P2VP}^k$  where  $k = (\alpha + 1)/3$ . As we have  $\alpha = 1.71$ ,  $k$  should be 0.9 which is the case. Therefore the results obtained by static and dynamic light scattering are in excellent agreement.

The characteristic exponents of  $N_{P2VP}$  dependence of the hydrodynamic radius to various models are 3/5, 2/3 and 1 for *hairy*, *crew-cut* and *amphiphile micelles*, respectively. Again the observed exponent is large and close to unity corroborating the fact that our case resembles to that of the *amphiphile micelles*.

### 3.3. Core size and corona thickness

Morphology studies were also performed by using transmission electron microscopy. In Fig. 8 electron micrographs of thin films of PS<sub>n</sub>P2VP<sub>n</sub> samples obtained from toluene solutions at room temperature are illustrated. In all cases we observed spherical micelles irrespective of the P2VP percentage. As the films were stained with iodine the observed dark spheres correspond to the cores of the micelles which are constituted from the P2VP arms of the heteroarm star copolymers. The sizes of the cores were determined from microtomes perpendicular to the surface of the films in order to avoid flattening effects taking place at the surface.

Micellar core radius are collected in Table 3. We observe that as the length of the P2VP arms increases the core size also increases. This is in agreement with the increase in the aggregation number of the micelles derived from LS measurements.

Assuming that the cores are free from solvent molecules,

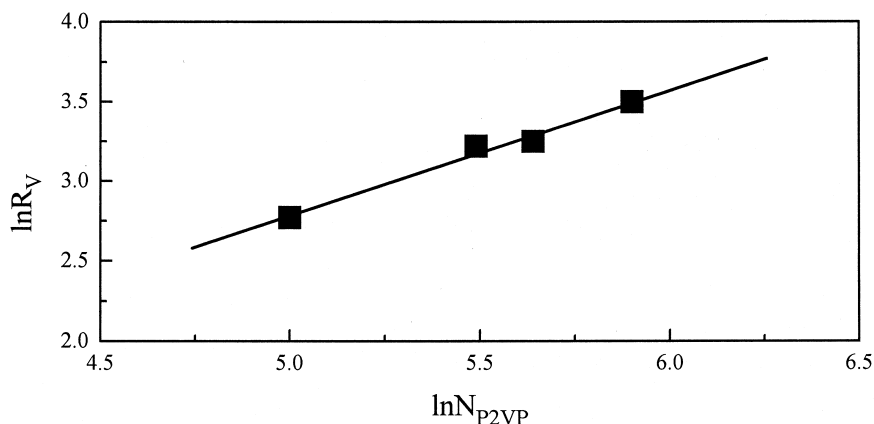


Fig. 6. Plot of the logarithm of the viscometric hydrodynamic radius as a function of the logarithm of the insoluble arm length.

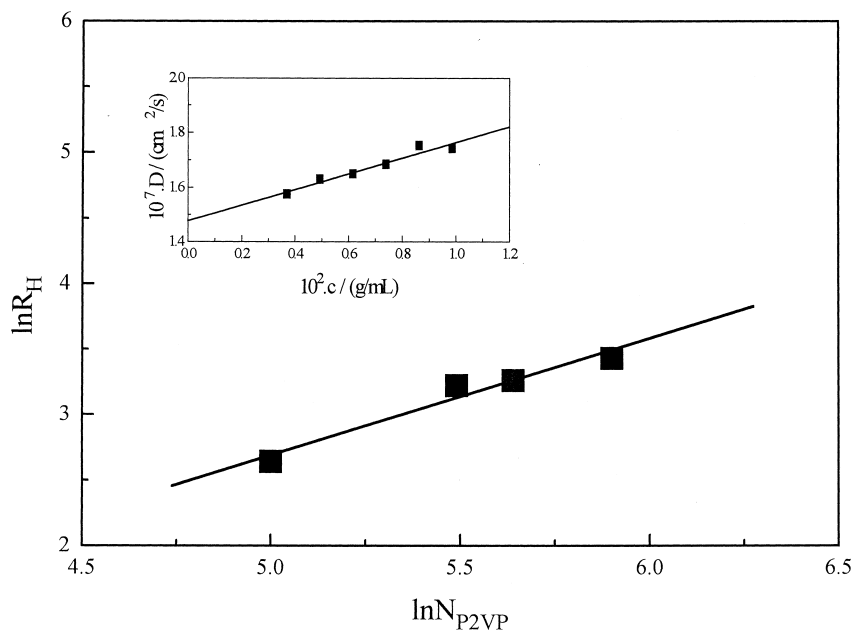


Fig. 7. Plot of the logarithm of the hydrodynamic radius as a function of the logarithm of the insoluble arm length. The inset demonstrates a typical plot of the diffusion coefficient versus concentration.

$R_c$  could be calculated from  $N_{agg}$  using the relation

$$\frac{4}{3} \pi R_c^3 = \frac{N_{agg} \cdot n \cdot N_{P2VP} \cdot m}{\rho N_{av}}, \quad (11)$$

where  $n$  is the number of the P2VP arms in each star molecule,  $m$  and  $\rho$  are the molecular weight and density of the VP monomer, respectively and  $N_{av}$  the Avogadro number. The calculated values are incorporated in Table 3. As it arises from the ratio of the experimental to the calculated values of the core radius, there is a satisfactory agreement between them. However the calculated values are always 1%–17% lower than the experimental ones. The highest deviation is observed for the lowest core radius where less accuracy in experimental determination is expected. As the calculated values from Eq. (11) are derived from other experimental values (i.e.  $N_{agg}$ ,  $n$ ) which also are subjected to experimental uncertainties we cannot decide whether the higher  $R_c$  experimental values arise from the presence of the solvent in the core or from experimental error.

As it is known the core radius of the micelles depends on both the length of the insoluble block and the length of the soluble block of the copolymer and can be expressed by scaling relations similar to Eq. (6) [19]:

$$R_c \sim N_{P2VP}^\delta N_{PS}^{-\epsilon}. \quad (12)$$

The  $N_{P2VP}$  dependence of  $R_c$  was determined by keeping  $N_{PS}$  constant and plotting the logarithm of  $R_c$  as a function of the logarithm of the number of the P2VP arm repeat units,  $N_{P2VP}$  (Fig. 9). A linear regression of the data with a correlation coefficient of 0.99 gave the scaling relation  $R_c \sim N_{P2VP}^{0.83}$ .

Again from Eqs. (11) and (12) the exponent  $\delta$  should be

equal to  $(\alpha + 1)/3$ , i.e. 0.9 while in our case  $\delta$  is slightly lower. However to our knowledge 0.83 is the highest exponent ever observed for diblock copolymer micelles. In some cases the reported values in the literature have been derived by using the calculated  $R_c$  values through Eq. (11). By using this procedure  $\delta$  was found to be 0.94 (with  $r = 0.997$ ) (graph not shown) which approaches further to unity, the predicted value for the *amphiphile micelles* [17].

Another interesting feature of the micellar cores is the degree of stretching,  $S_c$ , of the P2VP chains located inside the core.  $S_c$  is expressed as the ratio of micelle core radius to the P2VP chain end-to-end distance in the unperturbed state [20]

$$S_c = \frac{R_c}{(6.76 N_{P2VP})^{0.5} l}, \quad (13)$$

where  $l$  is the length of the VP monomer taken 0.25 nm. As  $R_c \sim N_{P2VP}^{0.83}$  then  $S_c$  should scale with the insoluble arm length as

$$S_c \sim N_{P2VP}^{0.33}. \quad (14)$$

Calculated  $S_c$  values are presented in Table 3. All the values are equal to or higher than unity implying that the P2VP chains are to some extent in the stretching form. Plotting  $S_c$  as a function of  $N_{P2VP}^{0.33}$  (graph not shown) a satisfactory linear dependence was found with a slope of 0.2 and correlation factor of 0.91 confirming Eq. (14). The aforementioned results demonstrated that the degree of stretching of the P2VP chains located on the core increases smoothly as the P2VP arm lengths increase. The opposite trend was observed for the polystyrene–poly(acrylic acid) copolymer micelles in aqueous solutions [20]. The latter could be

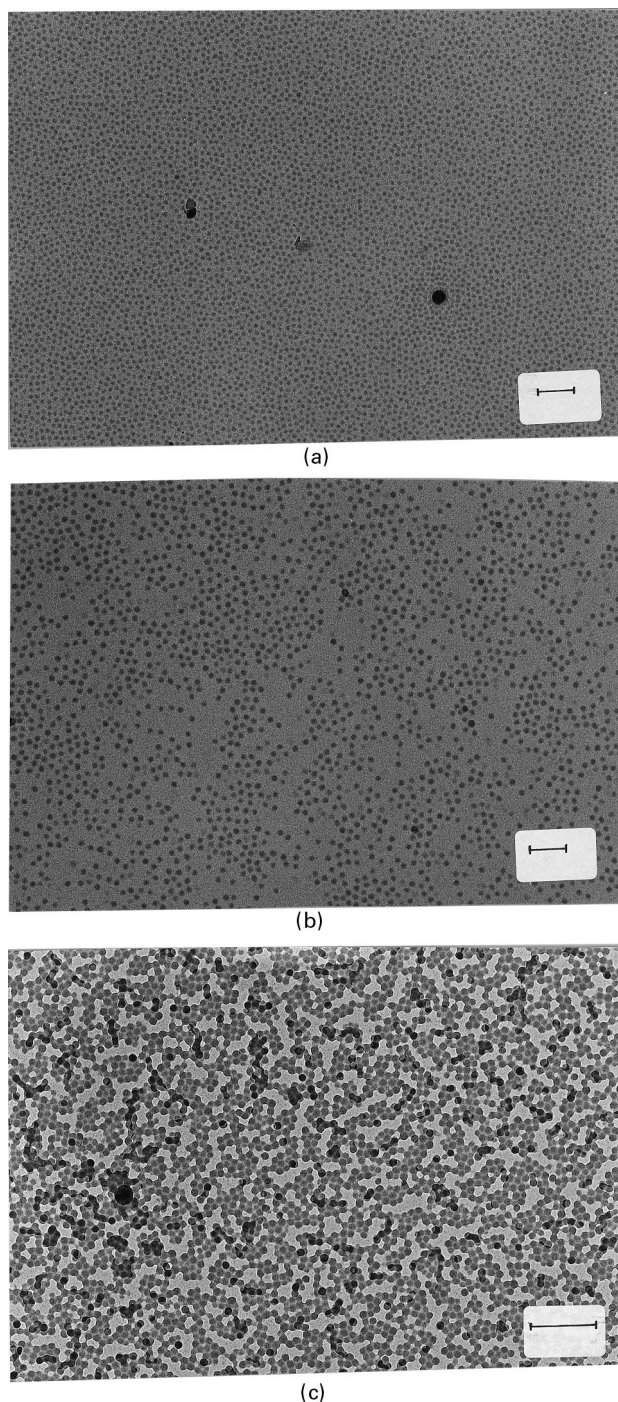


Fig. 8. TEM micrographs of (a)  $167_6-148_6$ , (b)  $167_6-282_6$  (the scale bar indicates 250 nm) and (c)  $167_6-365_6$  (the scale bar indicates 300 nm).

attributed to the weak dependence of the  $R_c$  with the insoluble block length, contrary to our case.

The determination of the core radius by TEM allows the calculation of the interchain distance,  $b$ . In the case of heteroarm star copolymers  $b$  is the distance between the neighboring nodules of the heteroarm star copolymers as these are located at the core–corona interface (see Fig. 1).  $b$  can be calculated from the core surface area per corona

star molecules according to the equation

$$4\pi R_c^2 = N_{\text{agg}} b^2. \quad (15)$$

For the *amphiphile micelles*, theory predicts  $N_{\text{agg}} \sim N_{\text{P2VP}}^2$  and  $R_c \sim N_{\text{P2VP}}$ . Therefore,  $b$  should be independent of the insoluble arm length. The  $b$  values given in Table 3 show practically no  $N_{\text{P2VP}}$  dependence with a mean value 11.8 nm. The inter-chain distance between those of the star molecules located at the core–corona interface is large as compared with the diblock copolymer systems. The  $b$  value is of the order of the end-to-end distance of free PS chains with the same degree of polymerization with the PS arms. This interfacial structure is because of the star-shape architecture of the macromolecules associated to micelles. As every six chain ends are gathered at the same point at the interface, an increased spacing between the interface molecules exists. A consequence of this is that some PS arms may be located parallel to the interface. Beyer et al. came to the same conclusion by exploring the interfacial area of lamellar morphologies afforded by polystyrene–polyisoprene heteroarm star copolymers [21].

Finally the corona thickness of the micelles were also evaluated from the equation  $L = R_H - R_c$  taking  $R_c$  either the experimental value or that calculated from Eq. (11). As shown in Table 3,  $L$  increases with the length of the insoluble arm although the length of the PS arms located at the corona was kept constant. This is because of the fact that the corona size depends on the insoluble arm length through its dependence on the aggregation number.

Linear regression analysis of double logarithmic plot of  $L$  as a function of  $N_{\text{agg}}$  gives the scaling relation  $L \sim N_{\text{agg}}^{0.54}$  ( $r = 0.93$ ) and/or  $L \sim N_{\text{agg}}^{0.46}$  ( $r = 0.97$ ) when calculated  $R_c$  values are used. In both cases the exponents are quite high compared with those obtained in diblock copolymers where the star model predicted 1/5 [22].

The different corona size for micelles constituted from soluble PS chains of the same length implies different chain conformations. In order to evaluate the degree of stretching of the PS chains (arms),  $L$  was compared to the end-to-end distance of free PS chains, which has the same degree of polymerization with the star arms, diluted in toluene, by using Eq. (16) established by Higo et al. [23]

$$R_0 = a\sqrt{6}N_{\text{PS}}^\nu, \quad (16)$$

where  $R_0$  is the root mean square end-to-end distance  $a = 0.186$  nm and  $\nu = 0.595$ . Values of the ratio  $L/R_0$  are collected in Table 3. The corona chains are in stretched form the degree of which increases with the aggregation number.

There is an exception. The  $L/R_0$  value for the micelles with the lowest corona thickness is lower than unity. This could be attributed to the fact that, in the micelles with the lowest core size, although  $b$  remains approximately constant the inter-chain space is even higher because of the higher curvature of the core surface. This implies that the corona

Table 3  
Core and corona structural characteristics of the PS<sub>n</sub>P2VP<sub>n</sub> heteroarm star copolymer micelles in toluene

Sample	$R_c$ (nm)	$R_{c,cal}^a$ (nm)	$R_c/R_{c,cal}$	$S_c$	$b$ (nm)	$L^b$ (nm)	$L/R_0$
167 <sub>6</sub> -148 <sub>6</sub>	8.0	6.8	1.17	1.01	12.7	6 (7.2)	0.73
205 <sub>6</sub> -240 <sub>6</sub>	12.0	11.3	1.06	1.19	11.0	13 (13.7)	1.35
167 <sub>6</sub> -282 <sub>6</sub>	12.5	12.3	1.01	1.14	11.4	13.5 (13.7)	1.41
167 <sub>6</sub> -365 <sub>6</sub>	17.5	16.0	1.09	1.41	12.1	13.5 (15)	1.51

<sup>a</sup> Calculated core radius using Eq. (11),  $\rho$  of vinyl pyridine was taken as 1.17 g/ml. From Ref. [25].

<sup>b</sup> Calculated value from  $L = R_H - R_c$  (values in parenthesis resulted by using  $R_{c,cal}$ ).

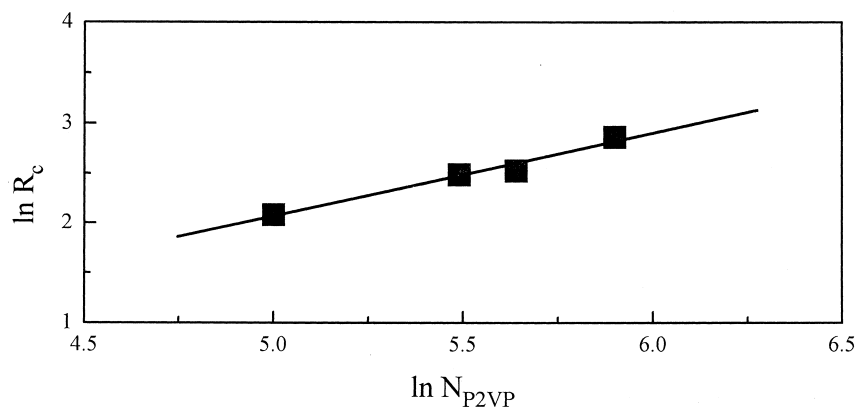


Fig. 9. Linear dependence of the logarithm of the core radius from the logarithm of the insoluble arm length.

chains are located closer to the core in an attempt to protect the insoluble parts of the micelles.

#### 4. Conclusions

In this article, the micellar behavior of PS<sub>n</sub>P2VP<sub>n</sub> heteroarm star copolymer micelles in toluene, which is a selective solvent for the PS arms of the star polymer, as a function of the length of the insoluble P2VP arm length,  $N_{P2VP}$ , was explored. All the micellar characteristics such as  $N_{agg}$ ,  $R_v$ ,  $R_H$  and  $R_c$  are strongly dependent on  $N_{P2VP}$ . This behavior has been expressed in scaling relations collected in Table 4. Comparing the calculated exponents with those concerning the various models for diblock copolymer micelles (i.e. *hairy*, *crew-cut*, *amphiphile micelles*) we conclude that our case belongs to the class of *amphiphile micelles* which

Table 4  
Scaling relations for the PS<sub>n</sub>P2VP<sub>n</sub> heteroarm star copolymer micelles in toluene

Relation	$r^a$	Exponent <sup>b</sup>
$N_{agg} \sim N_{P2VP}^{1.71}$	0.99	2
$R_v \sim N_{P2VP}^{0.8}$	0.99	1
$R_H \sim N_{P2VP}^{0.89}$	0.98	1
$R_c \sim N_{P2VP}^{0.83}$	0.99	1

<sup>a</sup> Regression coefficient.

<sup>b</sup> Theoretical exponents characteristic of *amphiphile micelles* model.

is characteristic for the micellization of strongly segregated amphiphilic systems such as PS-b-P4VP/toluene [13] and PS-b-PMA/dioxane–water [24]. It seems that the star-shaped architecture does not have significant effects on the scaling relations as they resemble those of PS-b-P4VP/toluene system which is a thermodynamically similar system. However differences were observed on the structure of the core–corona interfacial area as well as the influence of the insoluble arm length to the corona thickness.

In a further investigation we intend to study these PS<sub>n</sub>P2VP<sub>n</sub> polymers in aqueous solutions where the P2VP arms become water soluble at low pH.

#### References

- [1] Tuzar Z, Kratochvil P. *Adv Colloid Interface Sci* 1976;6:201.
- [2] Price C. In: Goodman I, editor. *Developments in Block Copolymers*, 1. Amsterdam: Elsevier, 1982:39.
- [3] Reiss G, Hurtez G, Bahadur P. In: *Encyclopedia of Polymer Science and Engineering*, 2nd ed. New York: Wiley, vol. 2, 1985:234.
- [4] Selb J, Gallot Y. In: Goodman I, editor. *Developments in Block Copolymers*, 2. Amsterdam: Elsevier, 1985:27.
- [5] Tuzar Z, Kratochvil P. In: Matijevic E, editor. *Surface and Colloid Science*, 15. New York: Plenum Press, 1993.
- [6] Alexandridis P, Hatton TA. *Colloids Surf A* 1995;96:1.
- [7] Tsitsilianis C, Kouli O. *Makromol Rapid Commun* 1995;16:591.
- [8] Tsitsilianis C, Papanagopoulos D, Lutz P. *Polymer* 1995;36:3745.
- [9] Voulgaris D, Tsitsilianis C, Esselink FJ, Hadziioannou G. *Polymer* 1998;39:6429.
- [10] Pispas S, Poulos Y, Hadjichristidis N. *Macromolecules* 1998;31:4181.

- [11] Pitsikalis M, Hadjichristidis N, Mays JW. *Macromolecules* 1996;29:179.
- [12] Iatrou H, Wilner L, Hadjichristidis N, Halperin A, Richter D. *Macromolecules* 1996;29:581.
- [13] Forster S, Zisenis M, Wenz E, Antonietti M. *J Chem Phys* 1996;104(24):9956.
- [14] Tsitsilianis C, Voulgaris D. *Macromol Chem Phys* 1997;198:997 and references there in.
- [15] Gao Z, Eisenberg A. *Macromolecules* 1993;26:7353.
- [16] Khougaz K, Gao Z, Eisenberg A. *Macromolecules* 1994;27:6341.
- [17] Zhulina EB, Birshtain TM. *Vysokomol Soedin* 1985;27:511.
- [18] Schulz MF, Khandpur KA, Bates FS, Almdal K, Martensen K, Hadjuk D, Gruner SM. *Macromolecules* 1996;29:2857.
- [19] Zhang L, Barlow BJ, Eisenberg A. *Macromolecules* 1995;28:6055.
- [20] Zhang L, Eisenberg A. *J Am Chem Soc* 1996;118:3168.
- [21] Beyer FL, Gido P, Poulos Y, Avgeropoulos A, Hadjichristidis N. *Macromolecules* 1997;30:2373.
- [22] Daoud M, Cotton JP. *J Phys (Paris)* 1982;43:531.
- [23] Higo Y, Ueno N, Noda J. *Polym J* 1983;15:367.
- [24] Qin A, Tian M, Ramireddy C, Webber SE, Munk P, Tuzar Z. *Macromolecules* 1994;27:120.
- [25] Webber RM, Anderson JL. *Langmuir* 1994;10:3156.